

**NANOSCALE BOEHMITE FILLER FOR CORROSION-
AND WEAR-RESISTANT POLYPHENYLENESULFIDE
COATINGS**

TOSHIFUMI SUGAMA

June 2003

Prepared for:
Office of Geothermal Technologies
U.S. Department of Energy
Washington, DC 20585

Under Contract No. DE-AC02-98CH10886

DISCLAIMER

This report was prepared as an account of work sponsored by an agency of the United States Government. Neither the United States Government nor any agency thereof, nor any employees, nor any of their contractors, subcontractors or their employees, makes any warranty, express or implied, or assumes any legal liability or responsibility for the accuracy, completeness, or any third party's use or the results of such use of any information, apparatus, product, or process disclosed, or represents that its use would not infringe privately owned rights. Reference herein to any specific commercial product, process, or service by trade name, trademark, manufacturer, or otherwise, does not necessarily constitute or imply its endorsement, recommendation, or favoring by the United States Government or any agency thereof or its contractors or subcontractors. The views and opinions of authors expressed herein do not necessarily state or reflect those of the United States Government or any agency thereof.

Available electronically at-

<http://www.doe.gov/bridge>

Available to U.S. Department of Energy and its contractors in paper from-

U.S. Department of Energy
Office of Scientific and Technical Information
P.O. Box 62
Oak Ridge, TN 37831
(423) 576-8401

Available to the public from-

U.S. Department of Commerce
National Technical Information Service
5285 Port Royal Road
Springfield, VA 22131
(703) 487-4650



Printed on recycled paper

**Nanoscale Boehmite Filler for Corrosion- and Wear-resistant
Polyphenylenesulfide Coatings**

Toshifumi Sugama

**Energy Resources Division
Energy Sciences & Technology Department
Brookhaven National Laboratory
Upton, NY 11973**

Keith Gawlik

**National Renewable Energy Laboratory
1617 Cole Boulevard
Golden, Colorado 80401**

This program report, issued by DOE Office of Geothermal Technologies, was performed under the auspices of the U.S. Department of Energy Washington, D.C. under Contract No. DE-AC02-98CH10866

TABLE OF CONTENTS

	Page
Summary.....	2
Introduction.....	3
Experimental Procedures	
Materials.....	4
Measurements.....	5
Results and Discussion	
Resistance to Blasting Wear.....	6
Thermal Behavior.....	7
300°C-autoclaved PPS.....	11
300°C-autoclaved Boehmite-filled PPS.....	13
Conclusion.....	16

LIST OF TABLES

Table 1. Typical chemical and physical properties of “as-received” boehmite filter.....	18
Table 2. XPS atomic fraction and atomic ratio of PPS film’s surfaces before and after exposure for 15 days in autoclave containing CO ₂ -laden brine at 300°C.....	18
References.....	19

LIST OF FIGURES

Figure 1. SEM image and EDX spectrum of “as-received” nanoscale boehmite cluster.....	21
Figure 2. Changes in the rate of blasting wear for the PPS coating’s surface as a function of boehmite	22
Figure 3. Cyclic DSC curve for the PPS coating.....	23
Figure 4. TGA curves for the 0,5, and 15wt% boehmite filled PPS films.....	24
Figure 5. FT-IR spectra for the 300°C-, 350°C-, 380°C-, 400°C-, and 420°C-heated PPSs.....	25

Figure 6. FT-IR spectrum of the PPS film after exposure in oven at 400°C....	26
Figure 7. Schematic representation of thermal oxidation pathway for PPS Film in temperature range 350°-440°C.....	27
Figure 8. XPS S_{2p} region for (a) unexposed PPS coating and (b) PPS coating after exposure for 15 days in CO₂-laden brine at 300°.....	28
Figure 9. FT-IR spectra for the PPS films before and after exposure for 15 days in CO₂-laden brine at 300°C.....	29
Figure 10. Backscattering SEM image and EDX spectra for the cross-sectional profile of 15wt% boehmite-filled PPS coating before exposure.....	30
Figure 11. Weight gain of boehmite-filled and unfilled PPS coatings deposited on primed carbon steel after exposure for up to 15 days in 300°C.....	31
Figure 12. XRD patterns for the 15wt% boehmite-filled PPS after (a) and before (b) exposure for 15 days at 300°C brine.....	32
Figure 13. Backscattering SEM image and EDX spectra for the cross- sectional area of 15wt% boehmite-filled PPS coating after exposure for 15 days in 300°C brine.....	33
Figure 14. Changes in pore resistance, R_p, for steel panels coated with boehmite-filled and unfilled PPSs as a function of exposure time.....	34

Summary

We evaluated the usefulness of nanoscale boehmite crystals as a filler for anti-wear and anti-corrosion polyphenylenesulfide (PPS) coatings exposed to a very harsh, 300°C corrosive geothermal environment. The boehmite fillers dispersed uniformly into the PPS coating, conferring two advanced properties: First, they reduced markedly the rate of blasting wear; second, they increased the PPS's glass transition temperature and thermal decomposition temperature. The wear rate of PPS surfaces was reduced three times when 5wt% boehmite was incorporated into the PPS. During exposure for 15 days at 300°C, the PPS underwent hydrothermal oxidation, leading to the substitution of sulfide linkages by the sulfite linkages. However, such molecular alteration did not significantly diminish the ability of the coating to protect carbon steel against corrosion. In fact, PPS coating filled with boehmite of $\leq 5\text{wt}\%$ adequately mitigated its corrosion in brine at 300°C. One concern in using this filler was that it absorbs brine. Thus, adding an excess amount of boehmite was detrimental to achieving the maximum protection afforded by the coatings.

Introduction

Our field tests at geothermal power plants demonstrated that no matter how and with what the internal surfaces of carbon steel heat exchanger tubes were coated with anti-corrosion and anti-fouling materials, fouling by geothermal brine-induced scale deposits still occurred at some different degrees^{1,2}. Among the technologies used for removing scales, hydroblasting at pressures ranging from 41.3 to 82.7 MPa is one commonly employed to clean heat exchanger tubes before their reuse. The major mineralogical constituents of the scales are silicate compounds and silica, raising concerns that when such scale-deposited surfaces are repeatedly cleaned by hydroblasting, the coating's surfaces undergo severe wear and tear. Such damage is due to the bombardment of the surfaces by dislodged hard mineral particles under velocity, causing topographical changes from smooth surfaces to rough ones. In the worst case, the liner film was completely worn out, so promoting the rate of corrosion of the underlying steel. In addition, the asperity of the coating's surfaces reinforced their strong physical affinity for the scales, thereby making it difficult to dislodge them. Consequently, an adequate resistance to blasting wear is required to extend the coating's useful lifetime as a corrosion-preventing barrier.

In our previous study on conferring resistance of poly(phenylenesulfide) (PPS) coating to blasting wear³, we incorporated an appropriate amount of aluminum oxide-rich calcium aluminate (ACA) as a filler into the PPS matrix. When the ACA-filled PPS coating was autoclaved in a simulated geothermal environment containing a low pH brine solution (1wt% sulfuric acid and 13wt% NaCl) at 200°C, the ACA fillers present in a superficial layer of ~ 65 μm thick favorably reacted with sulfuric acid in the brine that was permeating through the coating. This reaction led to the formation of well-formed boehmite crystals known to be hard, strong, engineering ceramic. Such in-situ growth of boehmite crystals coexisting with the PPS significantly improved the coating's resistance to blasting wear.

Recently, advanced nanoscale technology has made it possible to produce a nanosized boehmite crystal. An attraction in using such an extremely fine boehmite filler to replace the ACA filler is that the filled PPS coating's surfaces then may already have resistance to wear before exposing them in an autoclave. In other words, we can eliminate

the process of transforming the ACA filler into boehmite by exposing it to a hot brine solution.

The other intriguing question was whether this PPS-based coating would adequately protect the underlying carbon steel in a very harsh environment at a higher temperature of 300°C. Most of our studies of the PPS-based coatings thus far were devoted to investigating their value as corrosion-preventing barriers in 250°C hot brine⁴. We never have assessed their performance against corrosion in 300°C brine. Thus, our attention focused on the protective properties of nanoscale boehmite-filled PPS coating system in CO₂-laden brine at 300°C.

To obtain this information, we carried out the following five studies: (1) investigating the rate of blasting wear of the boehmite-filled PPS coating surfaces before exposure to hot brine; (2) determining the effects of boehmite filler on the coating's thermal properties; (3) examining the changes in chemical structure of thermally degraded and oxidized PPS as a function of temperature; (4) measuring the weight gain of boehmite-filled and unfilled PPS coatings after exposure in an autoclave at 300°C; (5) identifying the phases occupying the superficial layer of the exposed PPS coatings; and, (6) exploring the alternations of morphology and the changes in chemical composition for a cross-sectional profile of PPS coating after exposure. All the information was integrated and directly correlated with the data on the ability of the filled PPS to protect the steel against the 300°C brine-induced corrosion obtained from the recorded changes in conductivity of corrosive ions passing through the coating films as a function of exposure time.

Experimental Procedures

Materials

The nanoscale boehmite filler (Catapal® 200 Alumina) was supplied by Sasol North American Inc; Table 1 lists some of its chemical and physical properties. Figure 1 shows the secondary electron image of clustered nanosize boehmite filler taken by scanning electron microscopy (SEM), and its chemical elements detected from the energy-dispersive x-ray spectrometry (EDX). The metallic substrate used was commercial AISI 1008 carbon steel. A thermoplastic PPS powder with a particle size of <

60 μm was obtained from Ticona. It had a high melt flow at its melting point around 240°C. A 45wt% PPS powder was mixed with 55wt% isopropyl alcohol to make a slurry coating. Then, boehmite filler at 2, 5, 10, and 15% by weight of the total amount of PPS was added to the PPS slurry, and the mix was poured into a 110 ml shear blender. Mechanical blending for 2 min converted the agglomerated boehmite powder particles of $\sim 35 \mu\text{m}$ into a primary filler with particles of 100-500 nm; also, this uniformly dispersed the primary fillers in the slurry. Before depositing boehmite filler-incorporated slurries on the carbon steel coupons, their surfaces were covered with a zinc phosphate (Zn.Ph) primer by immersing them for 30 min into a phosphate solution, consisting of a 5.0 wt% zinc orthophosphate, 10.0 wt% phosphoric acid, 1.0 wt% manganese (II) nitrate hexahydrate, and 84.0 wt% water at 80°C. Then, the Zn.Ph-primed steel surfaces were rinsed with water at 25°C, and dried in an oven at 100°C for 30 min to remove any moisture. The resulting primer layer had ranged in thickness from a high of 55 μm to a low of 30 μm . It not only provides cathodic protection for the underlying steel against corrosion, but also enhances adhesion to the PPS coatings. The boehmite-filled PPS coating systems were deposited on the Zn.Ph-primed coupons in the following way. First, the primed coupons were dipped into the slurry, and withdrawn slowly. The slurry – covered coupons were left for 20 hours at atmospheric temperatures to volatilize the isopropyl alcohol, and simultaneously, to promote the conversion of the slurry layer into a sintering layer. Then, the sintered layer was heated in air at 310°C for 2 hours to achieve melt flow, and subsequently cooled to room temperature to make a solid film. This coating process was repeated twice more to assemble coating films, ranging from 280 to 320 μm thick. The thickness of coating films was determined from cross-sectional examination using scanning electron microscopy (SEM).

Measurements

The coated test panels (62.5 mm x 62.5 mm) were exposed for up to 15 days in an autoclave containing a CO₂-laden brine solution (0.5wt% sodium hydrogen carbonate, 13 wt% sodium chloride, and 86.5 wt% water) at 300°C under a hydrothermal pressure of 8.27 MPa. The blasting wear resistance of the surfaces of unexposed coatings was assessed using a silica (SiO₂) grit-blasting hand-held gun with 2 mm-diameter orifice

nozzle. The SiO₂ grits (particle size of 15 µm) were conveyed by a compressed air pressure of 0.62 MPa from a backpack hopper to the gun. From a standard distance of ~ 20 mm, the grits were projected for 2 min onto the coating surfaces at an angle of ~ 45°. The rate of wear was estimated as the loss in weight of the coatings (mg/min). Differential scanning calorimetry (DSC) and thermogravimetric analysis (TGA) were used to determine the changes in glass transition temperature and thermal decomposition temperature of the PPS matrix as a function of boehmite content. The alteration of the PPS's molecular structure caused by elevated thermal and hydrothermal temperatures was investigated using Fourier transform infrared (FT-IR). X-ray photoelectron spectroscopy (XPS) was used to assess the degree of hydrothermal oxidation and identify the chemical states formed on the oxidized coating's surfaces. The crystalline phases in the coating before and after exposure were identified using X-ray diffraction (XRD). SEM with the backscattering technique and energy-dispersive X-ray spectrometry (EDX) were employed to gain insights into the detailed state of the distribution of boehmite fillers dispersed in the PPS matrix, and to investigate morphological alterations of the coating after exposure for 15 days in a 300°C brine. AC electrochemical impedance spectroscopy (EIS) was used to evaluate the ability of the exposed coating films to protect the steel from corrosion. The specimens were mounted in a holder, and then inserted into an electrochemical cell. Computer programs were prepared to calculate theoretical impedance spectra and to analyze the experimental data. Specimens with a surface area of 13 cm² were exposed to an aerated 0.5 M sodium chloride electrolyte at 25°C, and single-sine technology with an input AC voltage of 10 mV (rms) was employed over a frequency range of 10 KHz to 10⁻² Hz. To estimate the protective performance of the coatings, the pore resistance, R_p, (ohm-cm²) was determined from the plateau in Bode-plot scans that occurred in low frequency regions.

Results and Discussion

Resistance to Blasting Wear

Figure 2 shows the rate of blasting wear for the 2, 5, 10, and 15wt% boehmite-filled and unfilled PPS coatings. The data clearly showed that the rate of wear of the unfilled PPS coating, at 1.04 mg/min, strikingly decreases with an increasing content of

boehmite. When 5wt% boehmite was incorporated into the PPS, the rate markedly dropped to 0.35 mg/min, corresponding to ~ three-fold reduction compared with that of unfilled coatings. Further, a reduction to 0.2 mg/min was obtained by adding 10wt%; beyond this content, the effect of more filler was little. Nevertheless, nanoscale boehmite fillers significantly enhance the resistance of PPS coating's surfaces to blasting wear.

Thermal Behavior

Figure 3 depicts the cyclic DSC curve of the unfilled PPS that encompasses two endothermic- and one exothermic-transition temperatures. The former endothermic reactions included the glass transition temperature, T_g , at the middle point of the downward slope between 98°C and 104°C, and the melting temperature, T_m . The latter was the crystallization temperature, T_c , representing the exothermic transformation of the molten state into a crystal state on cooling the melting polymer. Since the semi-crystalline PPS polymer structure contained two phases, amorphous and crystal, the T_g , called a second order transition, is related directly to some amorphous portions in which the main chains are not arranged and oriented. Hence, T_g is the temperature at which a physical characteristic of polymer changes from hard and brittle to soft and pliable⁵. In contrast, both the T_m and T_c , termed first order transitions, were implemented in the crystal portions; namely, the PPS melts when their crystal structure begins to fall apart, and become disordered molten state. This is the reason why PPS can have both a glass transition temperature and melting temperature. In other words, the amorphous portion undergoes the glass transition only, and the crystalline portion only undergoes melting. Correspondingly, the closed areas, A_c and A_m , of the exothermal and endothermal curves with the baseline represent the total latent heat energies, ΔH_c and ΔH_m , evolved or absorbed during crystallization and melting, respectively. The ΔH was computed using the following formula^{6,7}: $\Delta H = TRA/hm$, where T , R , A , h , and m refer to the temperature scale (°C in.⁻¹), the range sensitivity (mcal s⁻¹ in.⁻¹), the peak area (in.²), the heating rate (°C s⁻¹), and the sample's weight (mg), respectively.

Table 2 gives the changes in these thermal properties of PPS as a function of the boehmite content. Results showed that T_g increases with an increasing amount of boehmite. With 15wt% boehmite, the resulting T_g of 115°C was 14°C higher than that of

the unfilled PPS. Since, beyond the T_g , boehmite promotes the extent of relaxation and mobility of the segments in the molecular chains of the amorphous portions, the increase in T_g caused by incorporating more boehmite fillers seems to suggest that the fillers might act to immobilize and stiffen the chain's segments^{8,9}. One possible reason for the restriction in chain mobility and flexibility is the interactions at interfaces between the boehmite fillers and PPS's chains. In our previous study of the interaction between the aluminum oxide formed on aluminum metal's surfaces and the PPS¹⁰, we reported that it led to the formation of aluminum sulfate, $Al_2(SO_4)_3$, as the reaction product, reflecting the increase in bond strength at aluminum metal-to-PPS adhesive joints. Although we have no experimental evidence, if like aluminum oxide, the boehmite also reacts with PPS to form aluminum sulfate- or sulfide-related compounds, this may explain why segmental relaxation and mobilization behavior changed.

Regarding the T_m and T_c , the data showed that regardless of boehmite content, there were no significant changes in their peak temperatures; they ranged from 237° to 240°C for T_m and from 252° to 253°C for T_c . The values of both ΔH_m and ΔH_c decline with an increasing amount of boehmite. Knowing that the value of ΔH depends on the proportion of the crystalline PPS to boehmite, the drop in ΔH_m and ΔH_c values were primarily due to a decrease in this proportion with an increasing amount of boehmite. These findings demonstrate that boehmite nanofillers restrain the mobility and motion of chain's segments in the amorphous portions of PPS, but caused very little change in its crystalline arrangement.

Figure 4 depicts the TGA curves over the temperature range 300-700°C that highlights the thermal decomposition of the 0, 5, and 15wt% boehmite-filled PPSs in N_2 . The curve for the unfilled PPS (straight line) showed two stages of decomposition. The first pyrolytic decomposition began near 467°C, followed by a large loss in weight of ~ 47 % between 467° and 610°C; beyond this, in the second stage, weight loss gradually occurred between 610° and 700°C. When the features of curve for the 5wt% boehmite-filled PPS were compared with those of the unfilled PPS, there were two major distinctions. One was that the temperature of onset of decomposition increased 13°C to 480°C, and the other was that the total weight loss of at 700°C was ~ 46%. This weight loss was ~ 5 % less than that of the unfilled PPS at the same temperature. A further shift

in the onset temperature of decomposition to a higher value was observed for the 15wt% boehmite; at 700°C, weight loss was ~ 44%. As expected, this weight loss at 700°C depended upon the proportion of filler to PPS; namely, the lower weight loss can be attributed to a greater amount of filler. The line of DSC curve (not shown) for the 10wt% boehmite was located between the curves of 5 and 15wt% boehmite. The boehmite fillers appear to enhance the thermal stability of the PPS coatings. Relating these findings to the increase in the T_g value, such improved thermal stability may be due to the affinity of fillers for the PPS.

Based upon the TGA study, our attention next focused on the mechanisms of oxidative thermal decomposition of PPS, and the identification of its oxidation products over temperatures ranging from 300° to 420°C in air. To obtain these data, the PPS films, ~ 0.2 mm thick, were placed for 3 hours in an oven at 300°, 350°, 380°, 400°, and 420°C for FT-IR analysis, over the frequency range 4400-500 cm^{-1} (Figure 5). This information was expected to broaden out understanding of whether the PPS undergoes the brine-initiated hydrothermal oxidation and degradation in a 300°C autoclave, as well as clarify the degree of its oxidation, which is discussed later. At 300°C, a typical FT-IR spectrum of the PPS film included multiple absorption bands attributed to two groups, the aromatic rings at 3060, 1901, 1649, 1567, 1467, 1384, 1179, 1091, 1873, 1000, 961, and 814 cm^{-1} , and the sulfide linkage, C-S-C, at 744, 709, and 556 cm^{-1} ^{11,12}. In contrast, the spectrum at 350°C was characterized by the appearance of new band at 1232 cm^{-1} . According to the literature¹³, this new peak is ascribed to the sulfite group, -O-SO-O-, suggesting that the additional oxygen was incorporated into the PPS film at 350°C. Such incorporation led to the substitution of some sulfide linkages, which bind together the aromatic rings, by sulfite-type linkages as oxidative derivative of PPS. An increase in the heating temperature to 380°C resulted in the appearance of another two new bands at 1742 and 1655 cm^{-1} , revealing the formation of the aldehyde, -CHO, group, while the intensity of sulphite-related band at 1232 cm^{-1} conspicuously grew. Further growth of aldehyde- and sulfite-associated bands was seen in the spectrum at 400°C. Also, this spectrum showed a notable attenuation of the peak intensity related to all the aromatic rings and sulfide linkages, verifying that many of these groups within the PPS structure were transformed into oxidative derivatives. Several authors reported^{14,15}, in studies of the thermal and

photo-oxidation of polysulfone, that carbonyl oxidative derivatives were formed by oxidation of aromatic rings, reflecting the opening of the ring in the oxidation process. Thus, assuming that the rings in PPS also underwent an oxidation process similar to that observed in the polysulfone, this is the reason why the aldehyde derivative was formed. In other words, the attack of oxygen on the aromatic rings in PPS led to their opening, followed by the formation of the aldehyde group as one of the oxidative derivatives. From this information, it appears that the oxidation of aromatic ring and sulfide linkage in the PPS structure at temperatures of $\geq 380^{\circ}\text{C}$ can account for the formation of two oxidative derivatives, the aldehyde group and the sulfite linkage.

Spectral features of film heated at 420°C differed from those at 400°C , in particular, (1) the sulfite band at 1232 cm^{-1} became one of the dominant peaks, (2) the sulfide-related peaks disappeared, (3) the intensity of aldehyde peaks increased, and (4) a new band was present at 1449 cm^{-1} attributed to the sulfate, $-\text{O}-\text{SO}_2-\text{O}-$, linkage¹³. The formation of the sulfate linkage (4) can be taken as evidence that incorporating more oxygen not only promotes the extent of sulfide \rightarrow sulfite linkage substitution, $-\text{S}- \rightarrow -\text{O}-\text{SO}-\text{O}-$, but also causes the uptake of oxygen by sulfite, reflecting the replacement of the sulfite by the sulfate linkage, $-\text{O}-\text{SO}-\text{O}- \rightarrow -\text{O}-\text{SO}_2-\text{O}-$. Dramatic changes in spectral features were observed in the spectrum of the 440°C -heated PPS film (Figure 6), compared with that at 420°C . All the bands associated with the aromatic rings were eliminated, and new bands had developed at 1384, 1155, 797, 732, 656, and 609 cm^{-1} possibly due to the formation of sulfonic acid salt, $\text{R}-\text{SO}_2-\text{OH}$ ¹⁶. Another new band at 1091 cm^{-1} was attributable to the sulfinic acid salt, $\text{R}-\text{SO}-\text{OH}$ ¹⁶. Correspondingly, the OH group related to the band at 3425 cm^{-1} appeared to belong to the oxidized molecular fragments of these acid salts, while the band at 1625 cm^{-1} was caused by absorbed moisture. However, no study was made of the carbohydrate, R, to identify the precise formulas of these acid compounds. Nonetheless, this information strongly demonstrated that the oxidation at 440°C causes the breakage of two different bonds: one was the scission of the C-O bonds in the sulfite and sulfate linkages, and the other was the cleavage of the C-H bonds in the aromatic rings. Since the latter breakage abstracts hydrogen¹⁴, the acid salts may be formed by the interactions between the sulfite- and sulfate-based radicals, and the hydrogen.

From integrating all the data described above, in Figure 7, we schematically represent the thermal oxidation route of the PPS film at temperature ranges from 350° to 440°C.

300°C-autoclaved PPS

Before inquiring into the ability of boehmite-filled PPS coatings to avert the corrosion of carbon steel, our attention first turned to surveying the degree of hydrothermal oxidation of the PPS at 300°C, and also to investigating the changes in its molecular structure caused by oxidation. To obtain this information, the PPS films were exposed for 15 days in a 300°C autoclave containing CO₂-laden brine. The chemical composition and states occupying at the outermost surface site of unexposed and exposed films were surveyed by XPS to assess the degree of hydrothermal oxidation. FT-IR was used to provide the information on the conformational alteration of PPS. All XPS measurements were made at an electron take-off angle of 40°, which corresponds to an electron-penetration depth of ~ 5 nm, reflecting the detection of atomic compositions and chemical states present in a surface layer with a thickness of ~ 5.0 nm. The surfaces of exposed PPS films were rinsed with the deionized water to eliminate any contaminants before making the XPS survey. Table 2 gives the XPS atomic fractions of all the chemical elements detected on the surfaces of PPS films before and after exposure, and also includes the atomic ratio of O/S. Quantitative data for the respective chemical elements were estimated by comparing the XPS S_{2p}, C_{1s}, and O_{1s} core-level excitation peak areas, which then were converted into atomic concentrations. Before exposure, the chemical composition of bulk PPS coating surfaces consisted of 13.0 % sulphur, 81.6 % carbon, and 5.4 % oxygen. Two elements, sulphur and carbon, appear to be derived from the PPS, and the remaining oxygen element, in conjunction with some carbon, may be associated with organic and atmospheric contaminants, such as carbonyl, carboxylate, carbon dioxide, and carbon monoxide. In contrast, the superficial layer of PPS film revealed the incorporation of a substantial amount of oxygen during the 15-day exposure, reflecting an increase of 10.5 % in oxygen content, compared with that of the unexposed one. Correspondingly, the atomic ratio of O/S for the unexposed films rose ~ 6.6 times to

2.79 after exposure, suggesting that the PPS underwent some hydrothermal oxidation at 300°C.

We next focused on identifying the hot brine-induced oxidation products by inspecting XPS S_{2p} core-level photoemission spectra in conjunction with the FT-IR for the unexposed and 15-day exposed PPS films. Figure 8 compares the XPS S_{2p} spectra from these surfaces before and after exposure. In these spectra, the scale of the binding energy (BE) was calibrated with the C_{1s} of the principal hydrocarbon-type carbon peak, fixed at 285.0 eV as an internal reference standard. A curve deconvolution technique, using a DuPont curve resolver, was employed to substantiate the information on the sulfur-related chemical states from the spectrum of the carbon atom. For the unfilled coatings, the spectrum (a) of unexposed PPS surfaces indicated the excitation of a symmetrical single peak at 163.8 eV, originating from sulfide sulfur in PPS. When the PPS coating was exposed for 15 days, the features of the surface spectrum (b) were characterized by three additional peaks at the BE position of 164.5, 165.6, and 168.2 eV, although the sulfide sulfur peak at 163.8 eV still remained as the principal component. According to the literature^{17,18}, the possible contributors to the excitations at 164.5, 165.6, and 168.2 eV are the sulfur in the disulfide (-S-S-), the sulfoxide (>S=O) group, and the sulfite (-O-SO-O-) group, respectively, proving that the PPS had undergone hydrothermal oxidation. The peak at 164.5 eV also is attributable to the sulfur in the ≡S-O- bond. Regarding the appearance of the disulfide group, there is no experimental evidence whether phenylenedisulfide was formed directly or indirectly through the hydrothermal oxidation of PPS. The generation of sulfoxide and sulfite groups strongly supported the results from the early FT-IR study; namely, the bridging sulfide linkages were replaced by the oxidation-induced sulfite linkages. Additionally, since the atomic ratio of O/S in the sulfite group is 3, the O/S ratio of 2.79 obtained from the XPS atomic fraction for autoclaved film's surfaces (Table 2) appears to be associated with the formation of sulfite.

To support this information, the same sample as that used in the XPS study was analyzed by FT-IR (Figure 9). The specific spectral characteristic of the exposed PPS film was the appearance of pronounced band at 1232 cm⁻¹ marked by an arrowhead,

compared with the unexposed one. Since this new band denotes the sulfite linkage, we believe that some sulfide linkages within PPS were replaced by sulfite linkages during the 15-day exposure. However, no absorption band related to the disulfide linkages was detected in this spectrum, suggesting that although XPS showed the presence of disulfide linkages in the surface layer with ~ 5 nm thick, the amount of these linkages throughout the entire film of ~ 0.2 mm would be negligible.

300°C-autoclaved Boehmite-filled PPS

One intriguing question is how uniformly are the nanoscale boehmite fillers distributed in the PPS matrix after mixing in the shear blender. In response to this question, we explored the cross-sectional area of 15wt% boehmite-filled PPS coating by SEM microphotograph taken from the backscattering electron image (Figure 10). Two distinctive features can be seen: One is the bright area, characterized by a reticular-shaped network structure; the other was the dark area. The EDX spectrum (Figure 10, top) from this bright area had two strong elemental peaks, aluminum and sulfur. Since the sulfur is attributable to that in the PPS, the aluminum appears to belong to the boehmite fillers. In contrast, the EDX (Figure 10, bottom) of the dark area included one dominant sulfur signal and the three very weak elemental signals related to carbon, oxygen, and aluminum, suggesting that this dark area is the PPS matrix. Thus, the bright area can be accounted for the nanoscale boehmite fillers, signifying that the fillers were distributed uniformly in the PPS matrix.

Figure 11 plots weight gain against exposure times up to 15 days in a 300°C brine for unfilled and 2, 5, 10, and 15wt% boehmite-filled coating films deposited on the zinc phosphated steel panels. During the first 5 days of exposure, the weight gain depended primarily on the amount of boehmite filler; an increase in its amount resulted in an increase in the weight of the coatings. The weight gain of the unfilled PPS coatings was 0.02 %, demonstrating that some brine permeates into them. The gain in weight rose 2.3fold when 5wt% boehmite was incorporated into the bulk PPS coatings. The highest gain of 0.28 % was obtained from the 15wt% boehmite-filled coatings; it corresponded to ten times more than that of the unfilled ones. This finding suggests that the boehmite fillers absorb a certain amount of brine that permeates through the PPS layer. Such an

uptake by the boehmite fillers might explain why the exposed coatings containing substantial amounts had a higher weight gain. A further gain was seen in all the specimens, except for the unfilled one, when the exposure time was prolonged to 10 days. Between 10 and 15 days exposure, all filled coatings exhibited a very gradual uptake of brine. However, there is no data on whether uptake finally levels off or continuously increases.

To verify the absorption of brine, we inspected by XRD the 15wt% boehmite-filled PPS coating before and after autoclaving for 15 days (Figure 12). The XRD pattern over the diffraction range 0.154 – 0.884 nm (Figure 12, a) for non-autoclaved coating showed the presence of two crystalline components, PPS and boehmite. After autoclaving, the XRD tracing (Figure 12, b) clearly revealed the appearance of the additional d-spacing lines related directly to NaCl crystals, implying that the 300°C brine penetrated in the coating during the 15-day exposure. To investigate how deep the brine penetrated, we explored by SEM-EDX the cross-sectional area of exposed coating (Figure 13). The backscattering SEM image disclosed an interesting feature; in particular, the coating consisted of two layers. The first layer, denoted as “layer A”, was a bright-colored one extending to depths of ~ 113 μm from the top surfaces. It also contained many micron-sized pores, which were represented by dark dots. The EDX spectrum in this layer included the Na and Cl peaks attributed to the brine, demonstrating that it had permeated through a top layer, A, of ~ 113 μm . Below layer A at location of ~ 130 μm from the surface, the typical microstructure of the original boehmite-filled PPS coating was seen in the SEM image. In addition, the EDX spectrum showed no brine-associated elemental signals, such as Na and Cl. Their absence suggests that the brine had not penetrated layer B.

Therefore, the nanoscale boehmite fillers appear to absorb a certain amount of the brine. Thus, adding an excess amount of boehmite fillers to the PPS matrix caused the uptake of a great deal of brine by the fillers, allowing it to penetrate deeply into the coating layer. This is the major reason why the 15wt% boehmite-filled PPS coating gained the most weight after exposure. Although there is no experimental evidence, such a large absorption of the brine by boehmite fillers might create an internal expansion stress, which could lead to the generation of micro cracks. If this assumption is valid, the

copious numbers of micro-sized pores observed in the SEM image might be due to cracks generated by the fillers in the PPS matrix absorbing the brine.

This fact raised serious concerns about whether PPS coatings containing a large amount of boehmite fillers adequately protect the underlying steel against corrosion. AC electrochemical impedance spectroscopy (EIS) was used to obtain this information. On the overall Bode-plot curves [the absolute value of impedance $|Z|$ (ohm-cm²) vs. frequency (Hz)], (not shown), our particular attention was paid to the impedance value in terms of the pore resistance, R_p . This can be determined from the plateau in the Bode plot occurring at a sufficiently low frequency of 5×10^{-2} Hz. Figure 14 shows the plots of R_p at 5×10^{-2} Hz for the steel panels (size, 60 mm x 60 mm) coated with unfilled and boehmite-filled PPS as a function of exposure time up to 15 days in a CO₂-laden brine at 300°C. For all unexposed coating panels, the R_p value of these test panels ranged from a low of 5×10^{10} to a high of 8.5×10^{10} . When the unfilled and filled PPS coating panels were exposed, except 10 and 15wt% boehmite, their R_p values gradually fell with increasing exposure time. Since the R_p value reflects the magnitude of ionic conductivity generated by the electrolyte passing through the coating layer, a high R_p value means a low degree of permeation of the electrolytes into the coating films. Hence, extending the exposure time increased the rate of uptake of the electrolytes by these coatings. The data also show that the R_p value of the coating filled with the highest amount of 15wt% boehmite, in this test series, markedly declined with elapsed exposure time, from 7.2×10^{10} ohm-cm² before exposure to 8.8×10^7 ohm-cm² after 15 days exposure. This finding strongly demonstrates that incorporating an excess amount of boehmite enhances the rate of permeation of the electrolytes through the coating. In contrast, coatings filled with ≤ 5 wt% boehmite retained the R_p value of $> 10^{10}$ ohm-cm² after the 15-day exposure, strongly suggesting that although they were exposed in a very harsh brine environment at 300°C, their ability to protect the steel against corrosion was still effectively maintained. In other words, the incorporation of ≤ 5 wt% boehmite filler did not significantly diminish the coating's efficacy as corrosion-preventing barrier layer.

Relating this finding to our earlier results, we originally thought that the conformational changes in the PPS's molecular structure from sulfide linkages to sulfite linkages caused by its hydrothermal oxidation during the 15-day exposure at 300°C

might reduce the coating's ability to mitigate corrosion of the steel: however, the R_p value of 15-day-exposed PPS coating without the boehmite still indicated a high number at $\sim 1.9 \times 10^{10} \text{ ohm-cm}^2$, implying that oxidation-induced transformation causes very little decline in its ability, if any. Meanwhile, the major reason for the increased rate of permeability of brine thorough coatings containing an excess amount of boehmite is due mainly to its absorption by the large amount of filler in the PPS matrix. This absorption may create a porous microstructure in the coating layers, allowing the electrolytes to permeate easily through the coating.

Conclusion

Incorporating nanoscale boehmite fillers in the semi-crystalline polyphenylenesulfide (PPS) coatings offered two advantages: One was a significant enhancement of the resistance to abrasive wear; the other was an increasing thermal stability of the coating. In fact, in the former instance, the rate of blasting wear of the unfilled coating was reduced six times by adding 15wt% boehmite. The possible reason for the latter was due to the interaction between the amorphous portion within PPS's molecular structure and the boehmite's surfaces, thereby raising the glass transition temperature of the PPS.

The study of the changes in molecular structure of PPS caused by thermal oxidation over the temperature range 300-440°C revealed that an oxidation pathway with four steps. In the first step, the sulfide, -S-, linkages within PPS were substituted for the sulfite, -O-SO-O-, linkages at 350°C, and then at 380°C, the incorporation of further oxygen led to the secondary step representing the opening of aromatic ring, while the extent of the sulfide→sulfite substitution increased. A further rise in temperature to 420°C, the third step, replaced the sulfite linkages with sulfate, -O-SO₂-O-, linkages along with an increment in the rate of ring opening. Finally, these oxidation-induced compounds were converted into oxidized fragments at 440°C, such as sulfonic and sulfinic acid salts.

This information strongly suggested that the PPS matrix in the unfilled and filled coatings underwent a certain degree of the hydrothermal oxidation after exposing them for 15 days in brine at 300°C; this reflected the replacement of some sulfide linkages by

sulfite linkages. There was no opening of aromatic rings caused by severe oxidation of the PPS. Consequently, PPS coatings filled with $\leq 5\text{wt}\%$ boehmite filler adequately protected the carbon steel against corrosion by 300°C brine, demonstrating that the sulfide \rightarrow sulfite transformation which had placed within the PPS dose not significantly diminish its ability to protect the steel. However, one concern about using nanoscale boehmite fillers was their absorption of brine. Thus, adding excessive amounts of boehmite to the PPS was detrimental to the maximum performance of the barrier layer. In fact, adding $15\text{wt}\%$ boehmite filler caused a large gain of weight after exposure, and created a porous microstructure containing copious numbers of microsize voids, allowing the brine to permeate easily through the coating. Such voids may form due to the generation of an internal stresses caused by the uptake of a substantial amount of brine. Hence, the desirable amount of nanoscale boehmite used as the filler of anti-corrosion and anti-wear PPS coating should be no more than $5\text{wt}\%$.

Table 1. Typical chemical and physical properties of “as-received” boehmite filler.

Al ₂ O ₃ , %	80
Na ₂ O, %	0.002
Bulk density, g/l	500-700
Surface area (BET), m ² /g	100
Crystalline size, nm	~ 30
Agglomerated particle size, μm	~ 35

Table 2. XPS atomic fraction and atomic ratio of PPS film’s surfaces before and after exposure for 15 days in autoclave containing CO₂-laden brine at 300°C

Autoclave exposure	Atomic fraction, %			Atomic ratio, O/S
	S	C	O	
Before	13.0	81.6	5.4	0.42
After	5.7	78.4	15.9	2.79

References

1. Sugama, T., "Interfaces between geothermal brine-induced scales and SiC-filled polymer linings", *Geothermic*, 27 (1998) 387.
2. Sugama, T., Elling, D. and Gawlik, K., "Poly(phenylenesulfide)-based coatings for carbon steel heat exchanger tubes in geothermal environments", *J. Mater. Sci.*, 37 (2002) 4871.
3. Sugama, T. and Hayenge, P., "Boehmite-reinforced poly(phenylenesulfide) as a wear/corrosion resistant coating", *Polymers & Polymer Composites*, 8 (2000) 307.
4. Sugama, T. and Gawlik, K., "Milled carbon microfiber-reinforced poly(phenylenesulfide) coatings for abating corrosion of carbon steel", *Polymers & Polymer Composites*, 11 (2003) 161.
5. Shalaby, S.W., Turi, E.A. and Harget, P.J., "Crystalline copolyamides of β -(4-aminophenyl)-propionic acid and caprolactam", *J. Polym. Sci.*, 14 (1976) 2407.
6. Ray, C.S., Huang, W. and Day, D.E., "Crystallization kinetics of a lithia-silica glass: effect of sample characteristics and thermal analysis measurement techniques", *J. Am. Ceram. Soc.*, 74 (1991) 2449.
7. Kelton, K.F., "Estimation of the nucleation rate by differential scanning calorimetry", *J. Am. Ceram. Soc.*, 75 (1992) 2449.
8. Lipatov, Yu.S., "Dielectric relaxation in the surface layers of poly(methylmethacrylate) and polystyrene", *Vysomolekul. Soedin.*, 7 (1965) 1430.
9. Galperin, I., "Dynamic mechanical properties of a TiO₂-filled cross-linked epoxy resin from 20-90°C", *J. Appl. Polym. Sci.*, 11 (1967) 1475.
10. Sugama, T. and Carciello, N., "The protection of aluminum alloys in harsh, corrosive environments by oxidized polyphenylenesulfide coatings", *Polymers & Polymer Composites*, 3 (1995) 289.
11. Lenz, R.W. and Handlovits, C.E., "Phenylene sulfide polymers. II. Structure of polymers obtained by the macallum polymerization", *J. Polym. Sci.*, 53 (1960) 167.

12. Port, A.B. and Still, R.H., "Synthesis and characterization of poly(phenylenesulfide), poly(2-methylphenylenesulfide), and poly(2,6-dimethylphenylenesulfide)", *J. Appl. Polym. Sci.*, 24 (1979) 1145.
13. Bellamy, L.J., "The infrared spectra of complex molecules", Chapman and Hall, London, pp. 394-410, (1975).
14. Gesner, B.D. and Kelleher, P.G., "Thermal and photo-oxidation of polysulfone", *J. Appl. Polym. Sci.*, 12 (1968) 1199.
15. Rivaton, A. and Gardette, J.L., "Photodegradation of polyethersulfone and polysulfone", *Polym. Degrad. Stab.*, 66 (1999) 385.
16. Nakanishi, K. and Solomon, P.H., "Infrared Absorption Spectroscopy", Holden-Day, Inc., San Francisco, pp. 50-51, (1977).
17. Riga, J. and Verbist, J.J., "The disulfide group in organic compounds: Conformational dependence of core and valences sulfur electronic levels by x-ray photoelectron spectroscopy", *J. Chem. Soc., Perkin. Trans. II*, 10 (1983) 1545.
18. Lindberg, B.J., Hamrin, K., Johansson, G., Gelius, U., Fahlman, A., Nordling, C. and Siegbahn, K., "Molecular spectroscopy by means of ESCA II. Sulfur compounds", *Phys. Scrip.*, 1 (1970) 286.

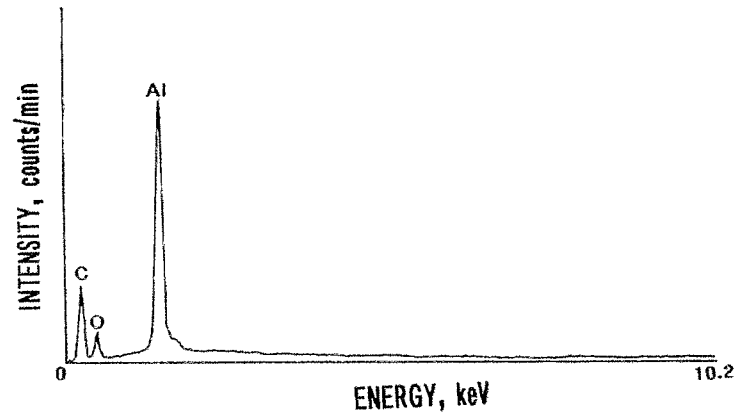
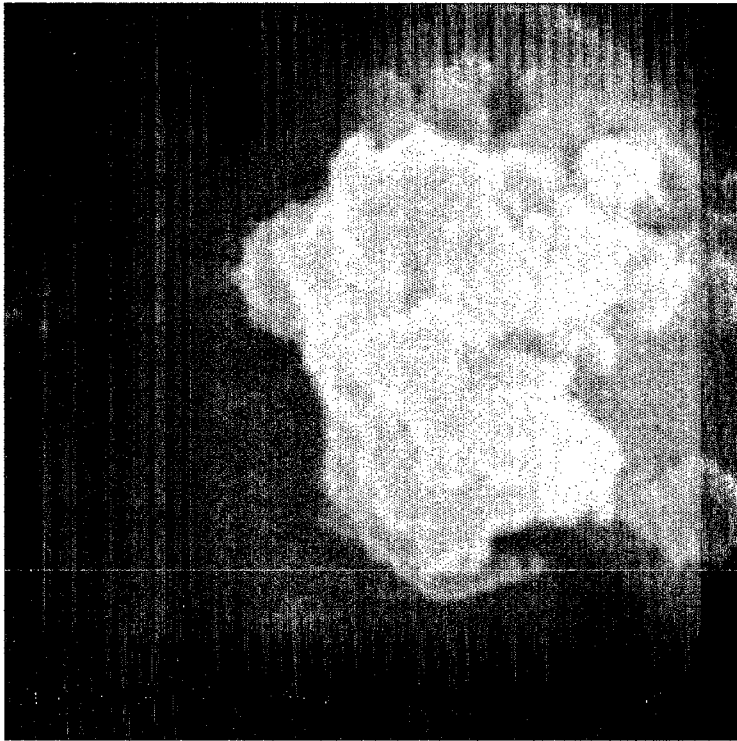


Figure 1. SEM image and EDX spectrum of “as-received” nanoscale boehmite cluster.

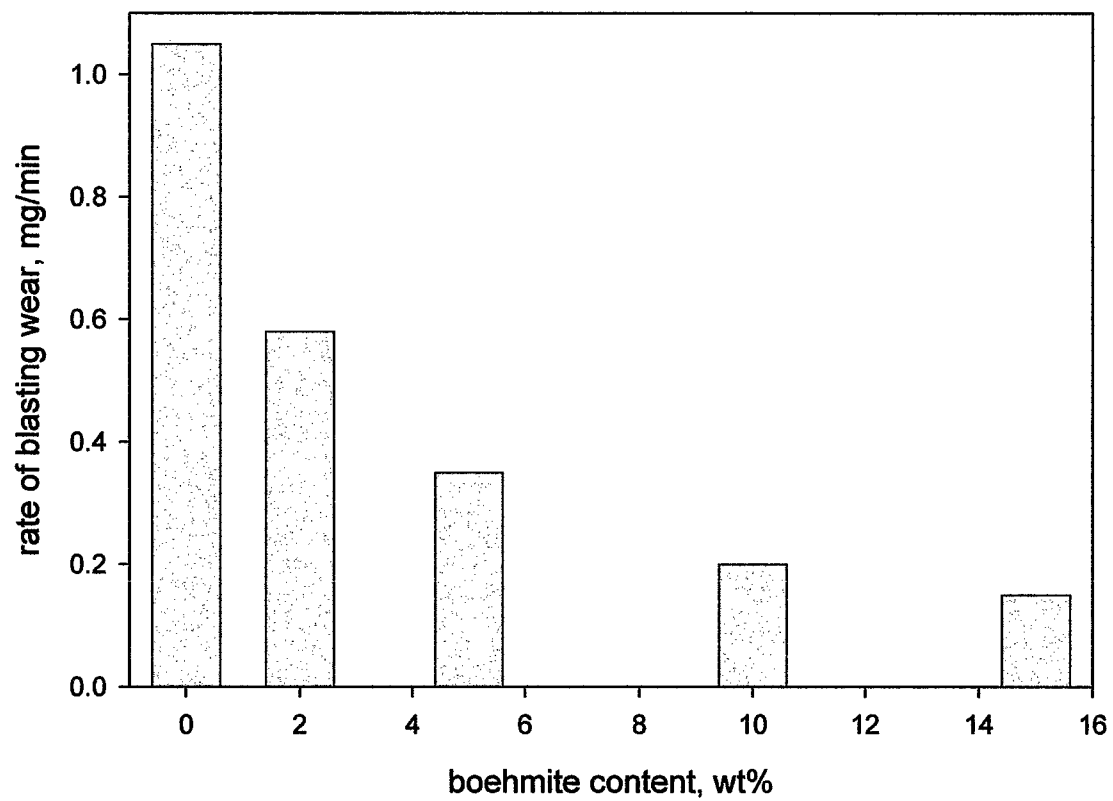


Figure 2. Changes in the rate of blasting wear for PPS coating's surface as a function of nano-scale boehmite filler content.

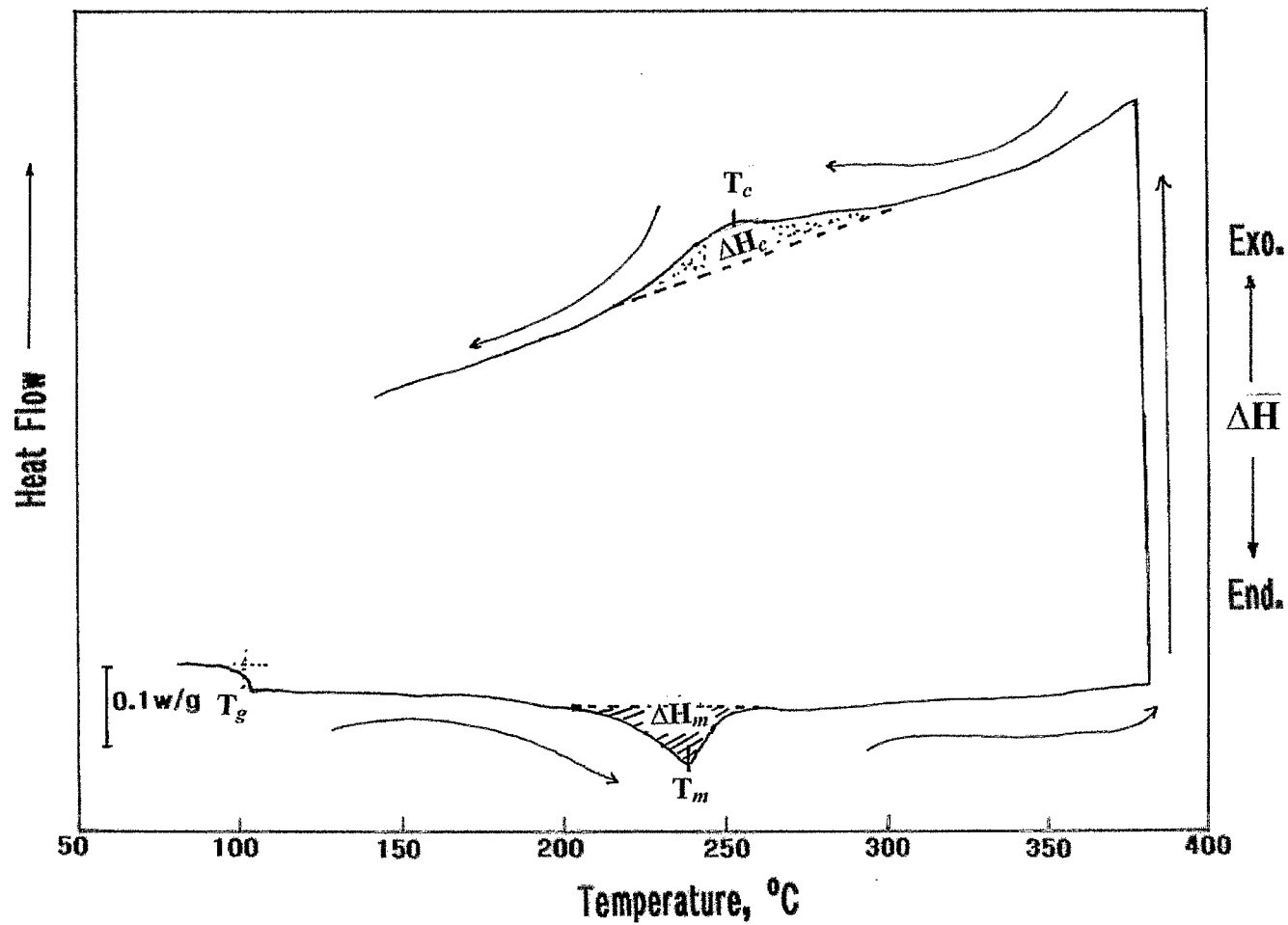


Figure 3. Cyclic DSC curve for the PPS coating.

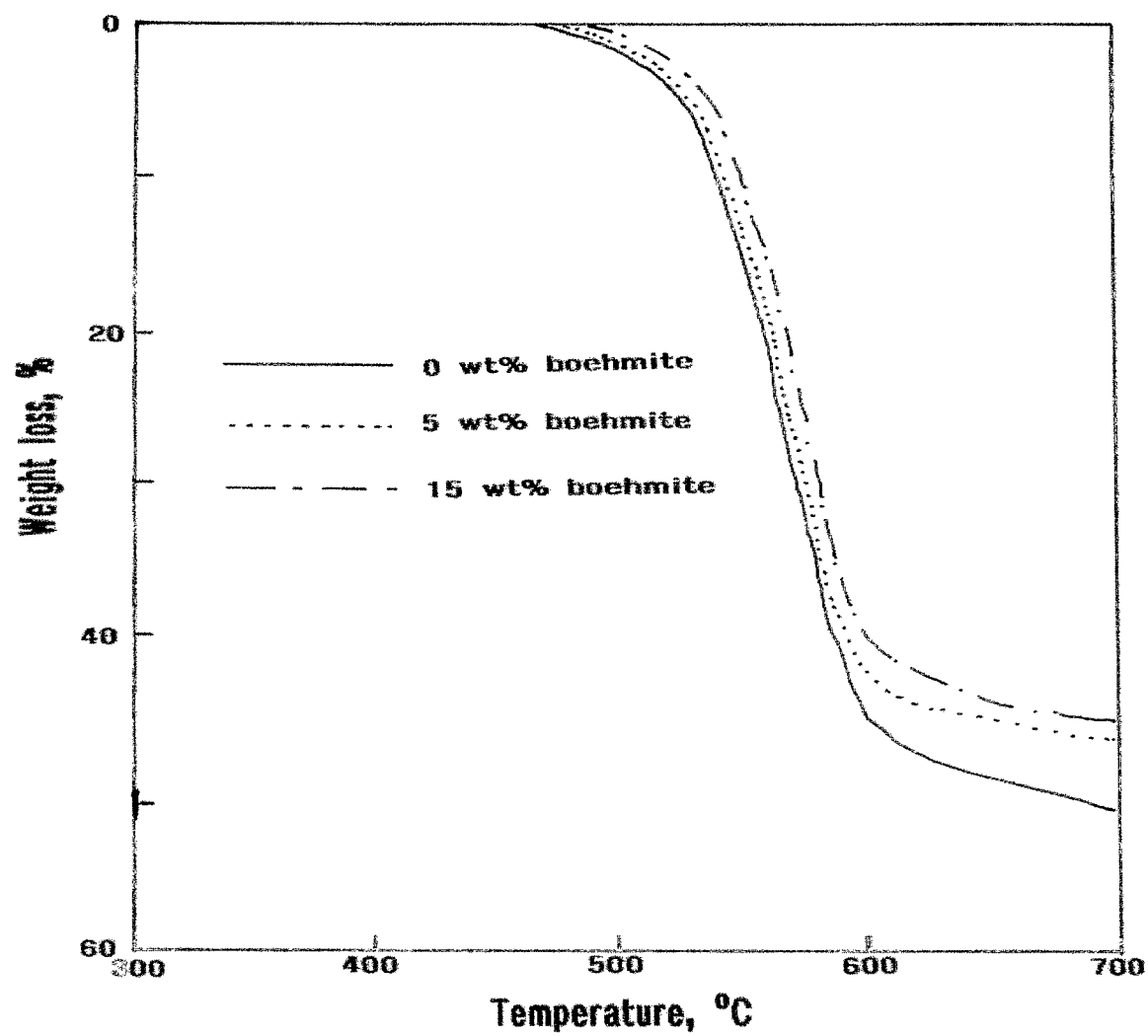


Figure 4. TGA curves for the 0, 5, and 15wt% boehmite-filled PPS films.

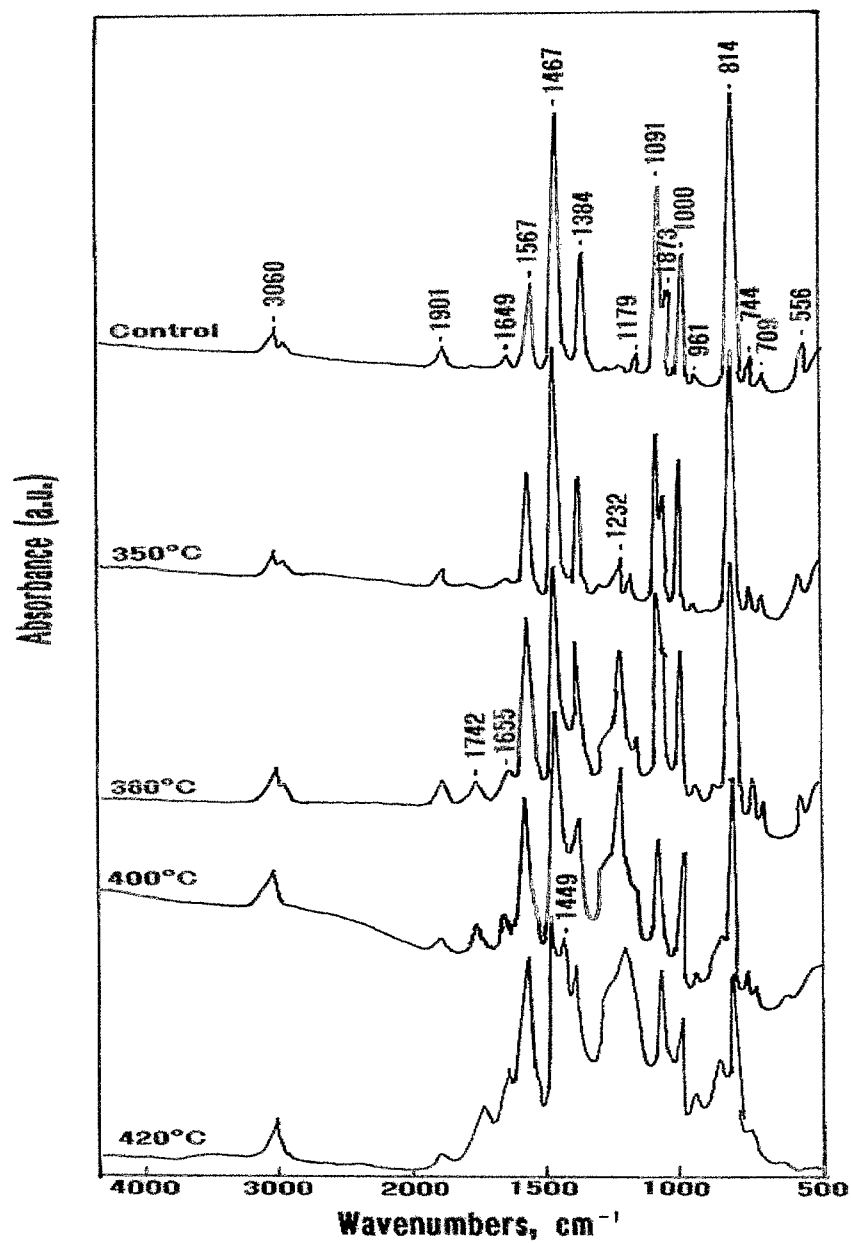


Figure 5. FT-IR spectra for the 300°C-, 350°C-, 380°C-, 400°C-, and 420°C-heated PPSs.

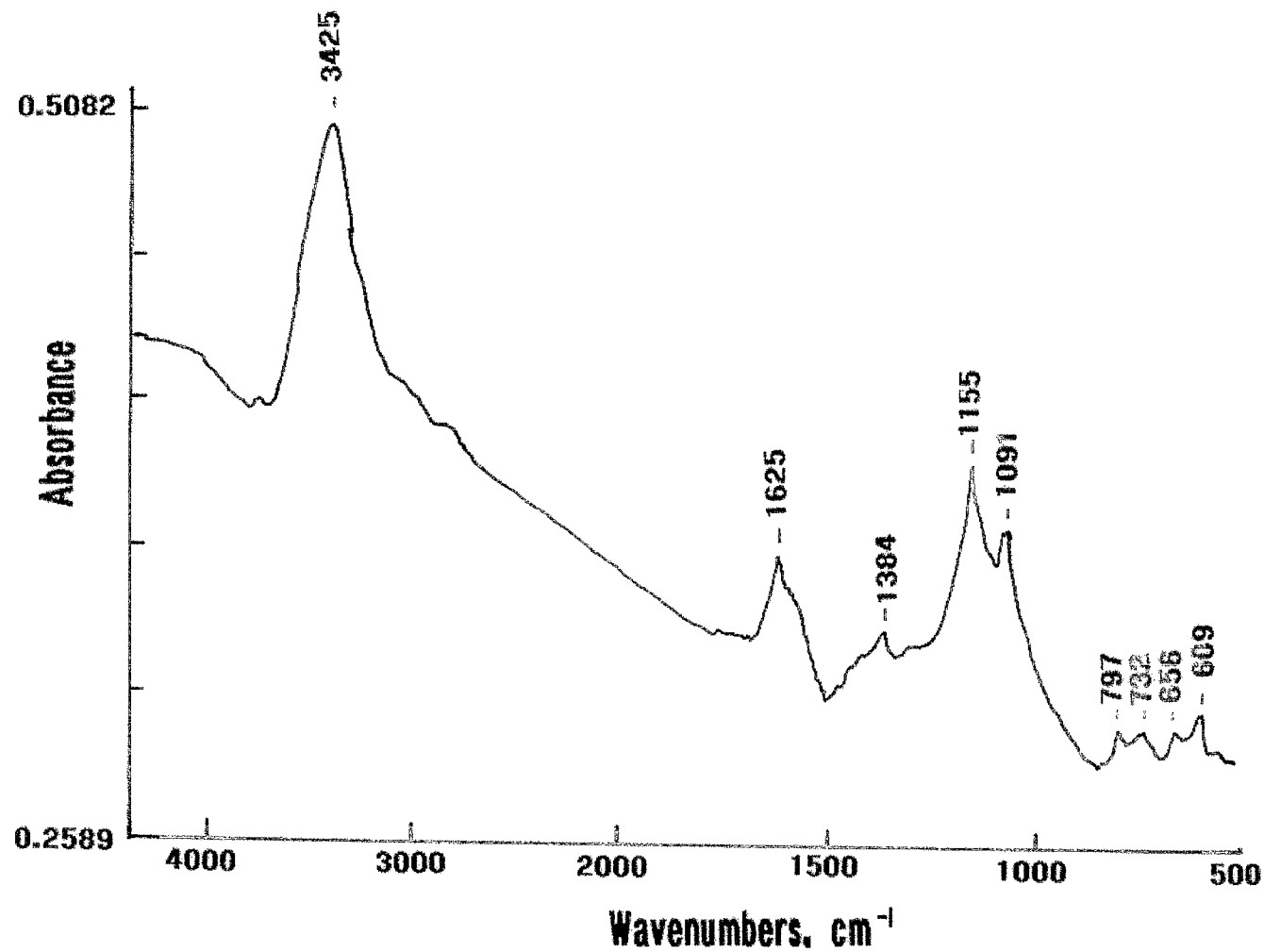


Figure 6. FT-IR spectrum of the PPS film after exposure in oven at 440°C.

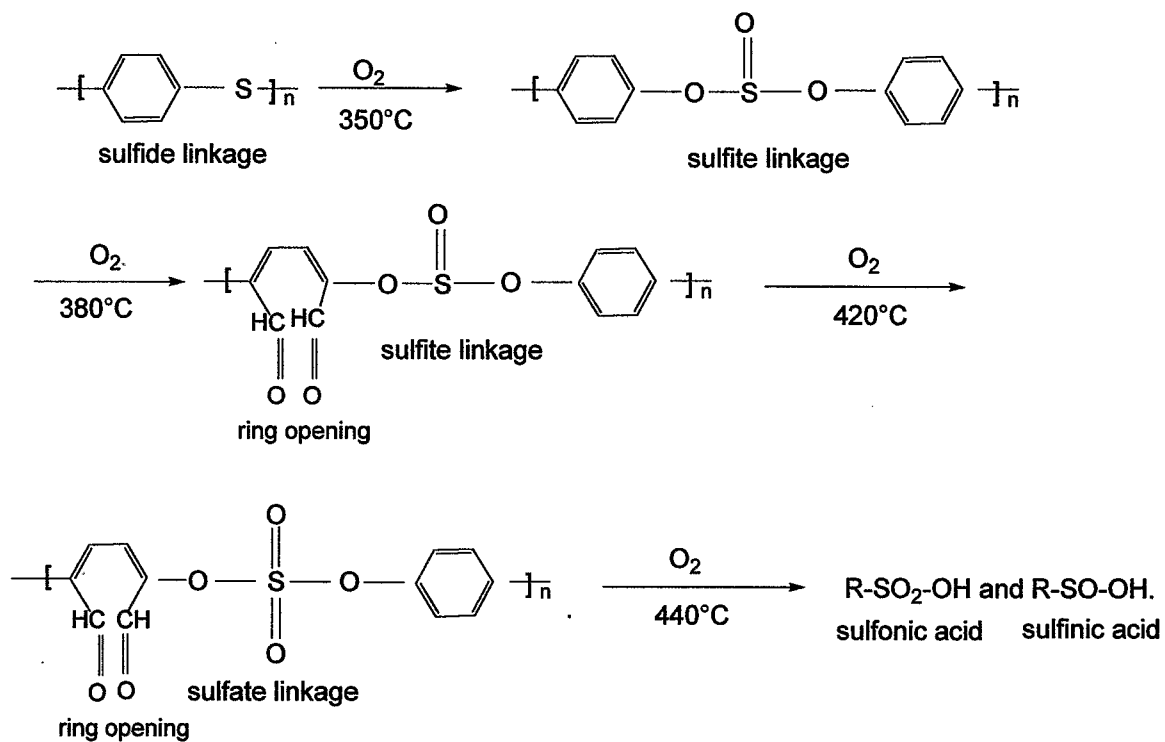


Figure 7. Schematic representation of thermal oxidation pathway for PPS film in temperature range 350° - $440^\circ C$.

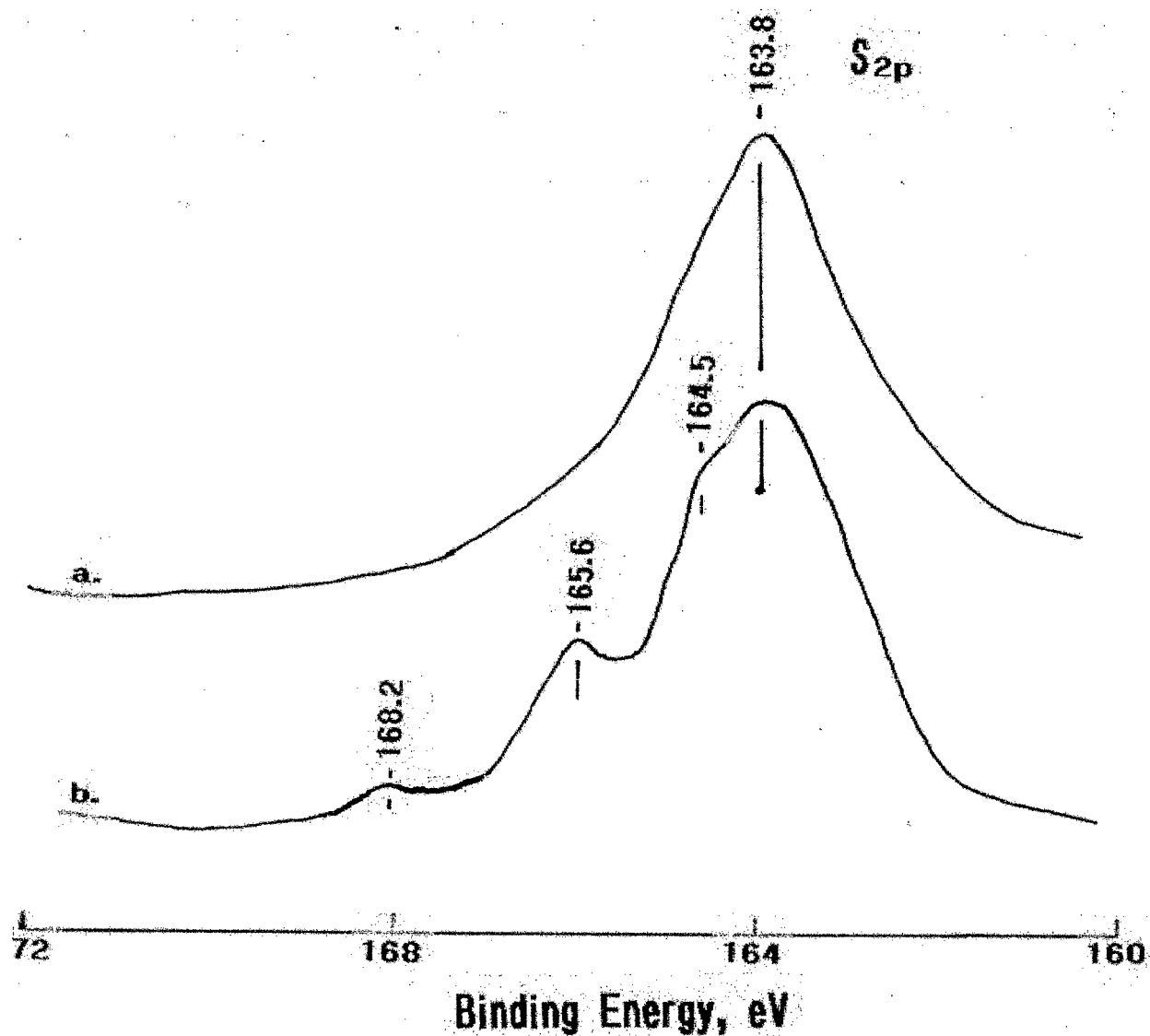


Figure 8. XPS S_{2p} region for (a) unexposed PPS coating and (b) PPS coating after exposure for 15 days in CO₂-laden brine at 300°C.

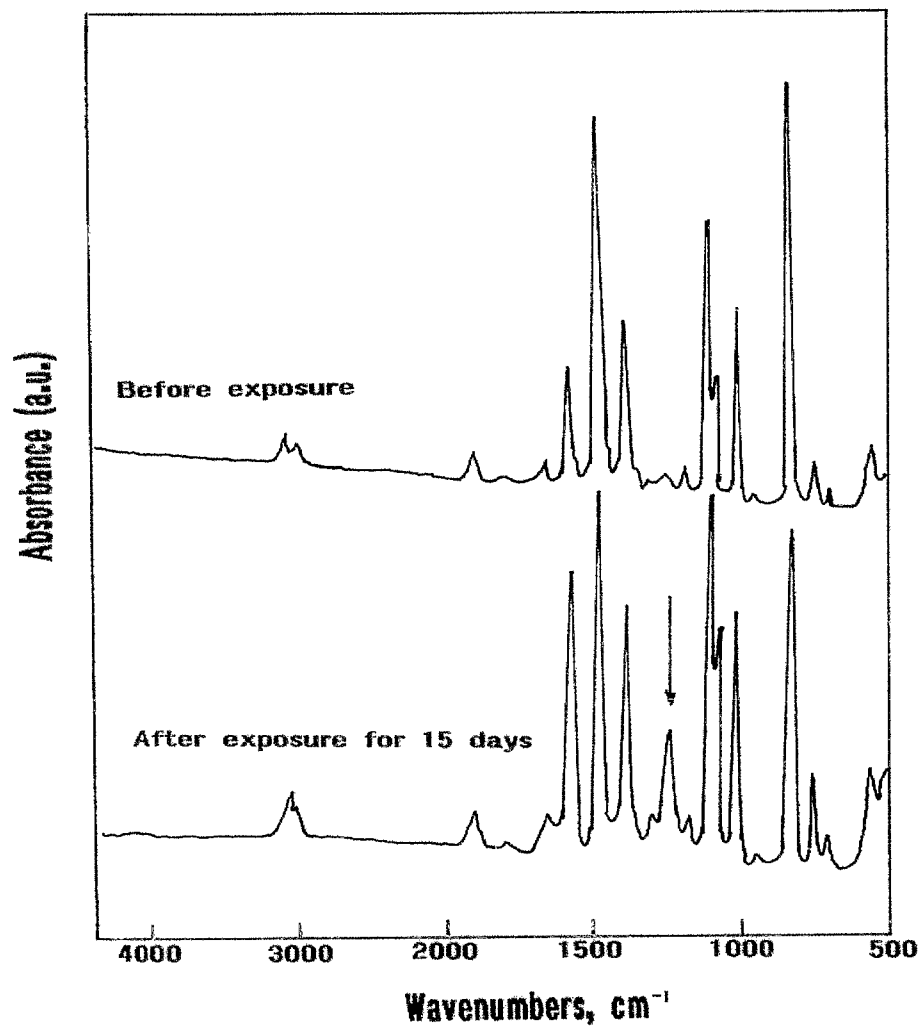


Figure 9. FT-IR spectra for the PPS films before and after exposure for 15 days in CO₂-laden brine at 300°C.

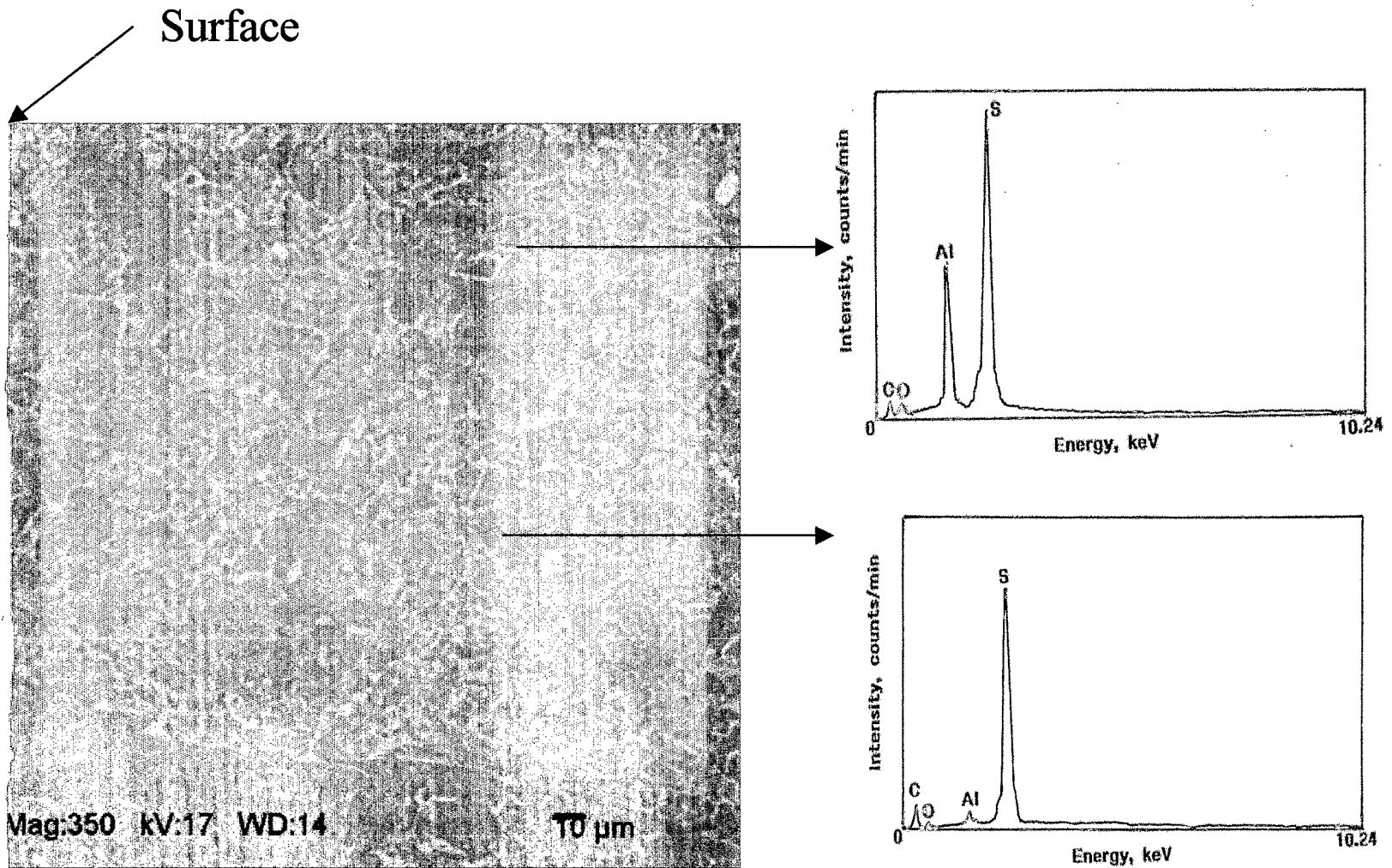


Figure 10. Backscattering SEM image and EDX spectra for the cross-sectional profile of 15wt% boehmite-filled PPS coating before exposure.

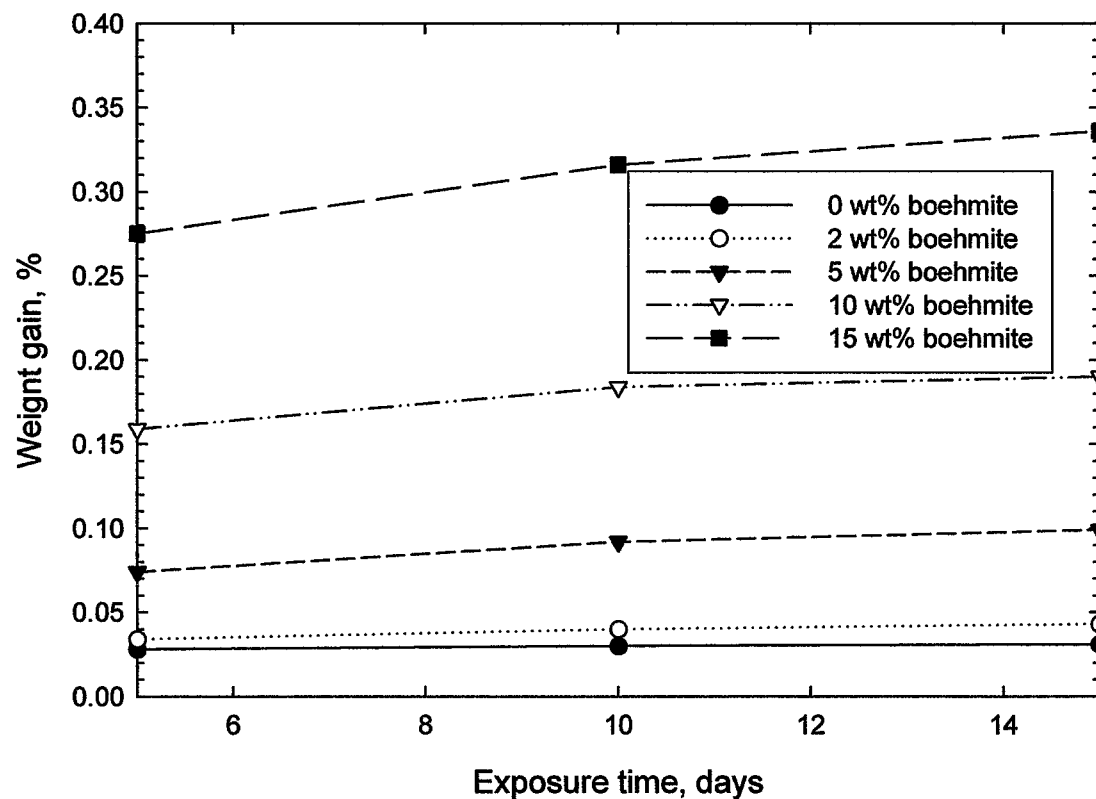


Figure 11. Weight gain of boehmite-filled and unfilled PPS coatings deposited on primed carbon steel after exposure for up to 15 days in a 300°C brine.

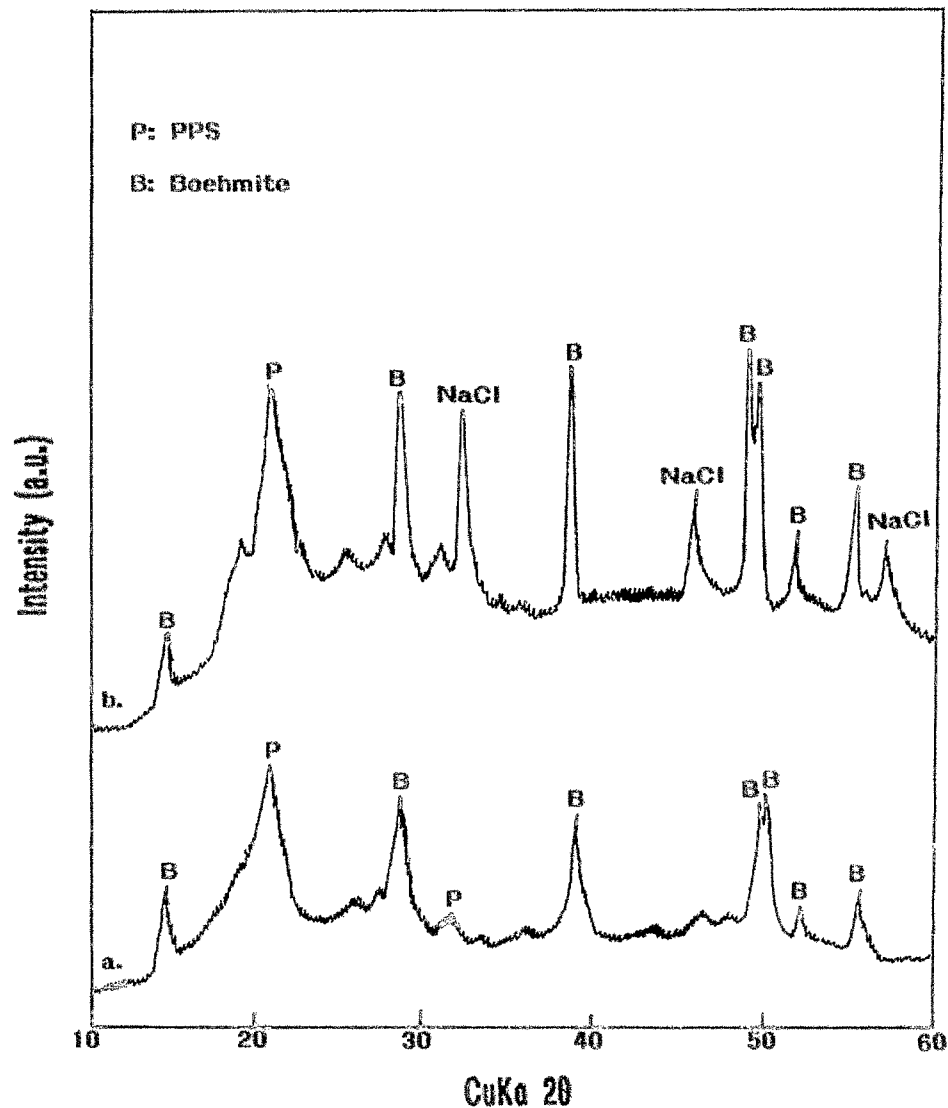


Figure 12. XRD patterns for the 15wt% boehmite-filled PPS after (a) and before (b) exposure for 15 days at 300°C brine.

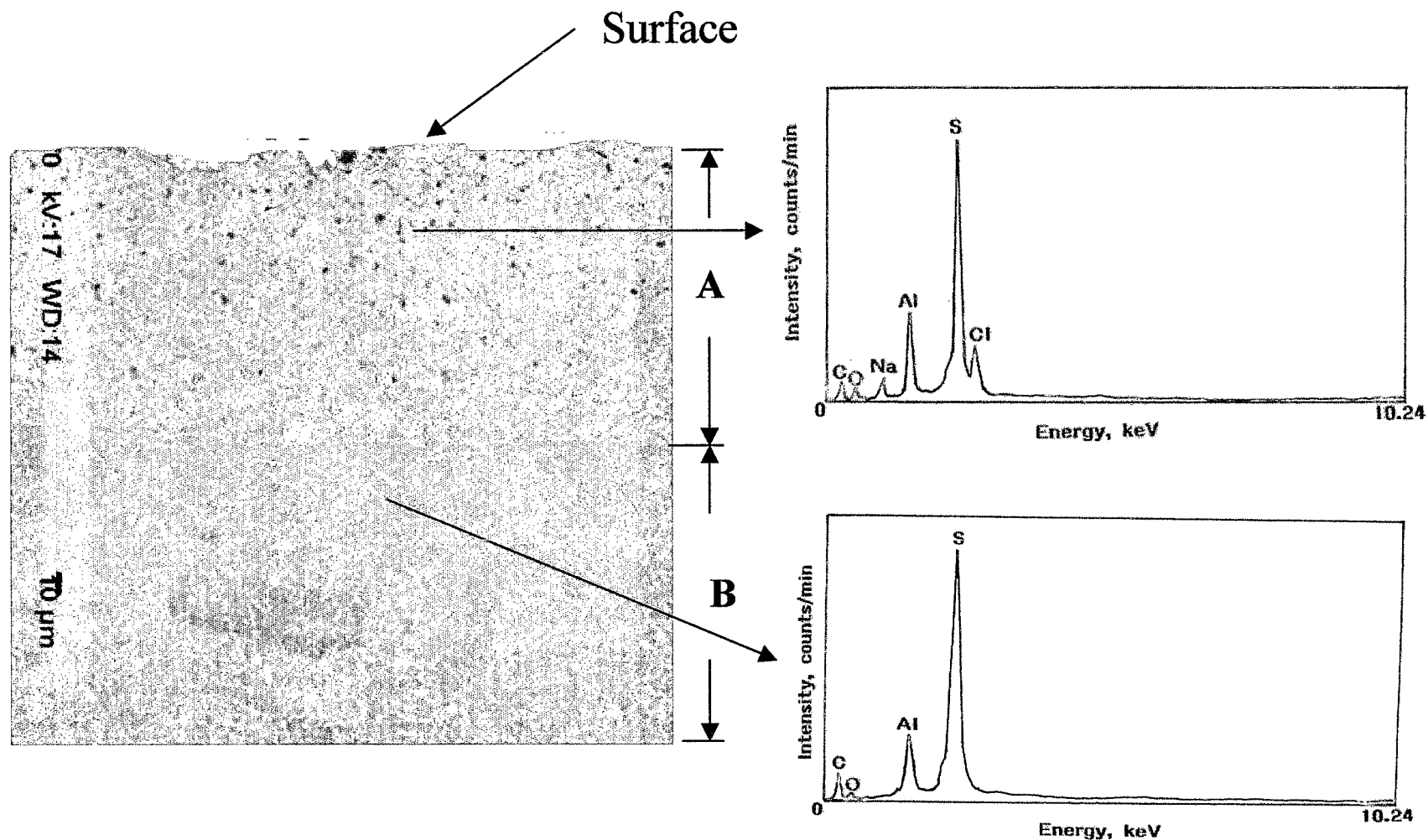


Figure 13. Backscattering SEM image and EDX spectra for the cross-sectional area of 15wt% boehmite-filled PPS coating after exposure for 15 days in 300°C brine.

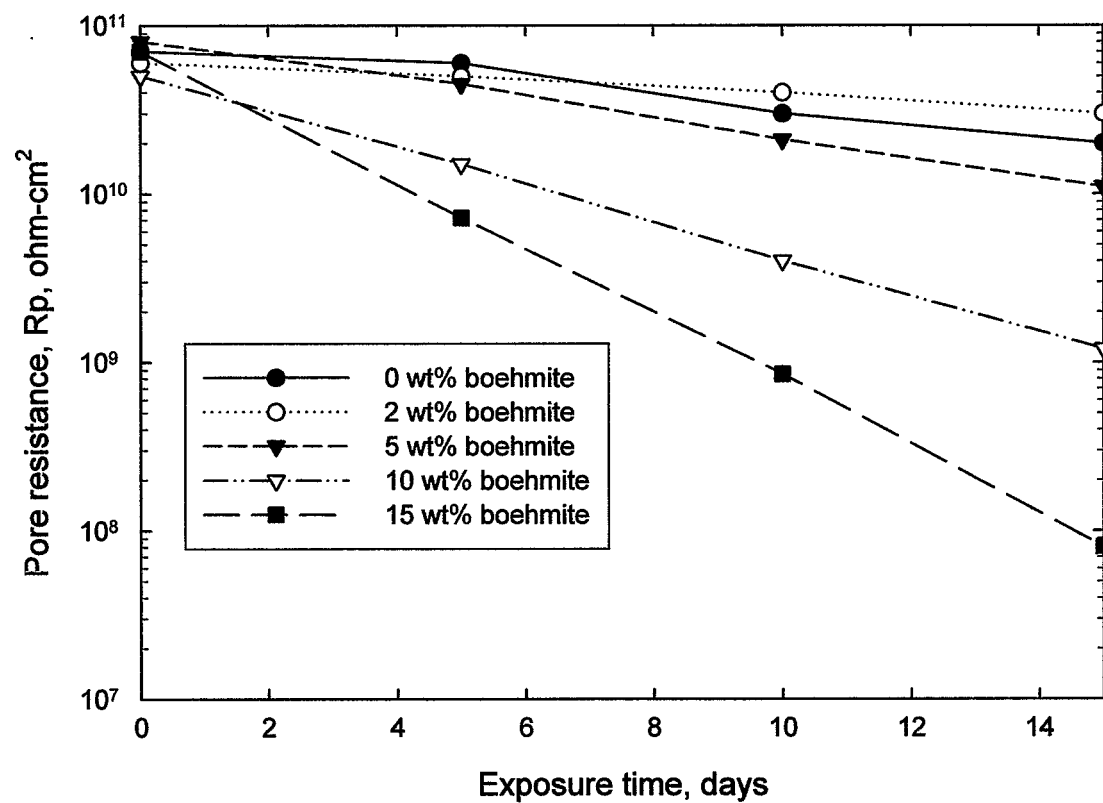


Figure 14. Changes in pore resistance, R_p , for steel panels coated with boehmite-filled and unfilled PPS as function of exposure time.